Using the Attainable Region Analysis to Determine the Effect of Process Parameters on Breakage in a Ball Mill

Matthew J. Metzger and Sachin P. Desai
Dept. of Chemical and Biochemical Engineering, Rutgers, The State University of New Jersey, Piscataway, NJ 08854

David Glasser and Diane Hildebrandt
Centre of Materials and Process Synthesis, University of the Witwatersrand, School of Chemical and Metallurgical Engineering, Johannesburg, Gauteng, South Africa

Benjamin J. Glasser
Dept. of Chemical and Biochemical Engineering, Rutgers, The State University of New Jersey, Piscataway, NJ 08854

DOI 10.1002/aic.12792
Published online October 28, 2011 in Wiley Online Library (wileyonlinelibrary.com).

Ball milling is one of the most common unit operations used for size reduction across a range of industries. However, it is also a notoriously inefficient process, often contributing substantially to operational costs. In this work, we investigate the influence of rotation rate, grinding media fill level and grinding media size on the optimal production of a product of intermediate size. We find that changing the grinding media size at otherwise identical conditions produces different breakage products as well as nonmonotonic trends with varying rotation rate and grinding media fill levels. In addition, we show how to use the attainable region analysis to explore the parameter space in a reduced time without having to perform tests at every parameter combination. Finally, we examine how the complex interplay between rotation rate, grinding media fill level and grinding media size can control the mechanism of breakage occurring inside a ball mill. © 2011 American Institute of Chemical Engineers *AIChE J,* 58: 2665–2673, 2012
Keywords: comminution, optimization, attainable region, grinding media size, breakage mechanisms, particulate processes

Introduction

Comminution, an operation to reduce the size of particles through an applied force, is essential to make products ranging from pigments for paints, to asphalt for road pavement to drug crystals for pharmaceutical tablets. It is estimated that the comminution industry utilizes over 6% of the entire world's energy.[1] Because of its simplicity and versatility, the ball mill is one of the most commonly encountered comminution devices. However, the ball mill is also one of the most inefficient size reduction devices, with the best estimates of the conversion of supplied energy into new surface creation ranging from 0.6[2] to 25%.[3] Therefore, at these current levels, the majority of the energy supplied to the process is lost to heat, noise, or other wasteful mechanisms. As a result, even the slightest increase in the efficiency of ball mill operation can offer a tremendous decrease in the energy usage of the comminution industry.

Breakage within a ball mill proceeds through three primary mechanisms.[4,5] Each mechanism results in a different product size distribution and is related to how energy is applied to the particle to be broken. Highly energetic collisions leading to complete destruction of the particle and wide product size distribution of product size is called "massive fracture." Low energy collisions resulting in minimal breakage is referred to as "attrition" or "abrasion," where one large particle similar to the size of the original particle remains along with many smaller particles called fines. "Cleavage" is the result of moderate energy impacts applied over a long period of time and produces a narrow distribution of particle sizes. The disparity of flow profiles of the grinding media and the particles inside a ball mill produces a wide range of collision energies,[6] meaning that each of the breakage mechanisms may be occurring simultaneously. However, properly tuning the operating conditions can lead to situations where one mechanism dominates the breakage leading to more consistent and thus more efficient operation.

As the type of breakage is controlled by the energy of the impact, the energy possessed by the grinding media is essential to determine how a particle will break. It may be obvious that the size of the grinding media has an influence over the impact energy, yet most ball mill design and scale-up equations only refer the total amount of grinding media and not the media size.[2,7,8] Recent experimental[9,10] and numerical[11] works have demonstrated the influence of the grinding media particle size on breakage in ball mills, suggesting a trade-off between the energy of each contact and the number of those contacts. Equations to determine the optimal grinding media size do exist in the literature but they are lacking in many respects. Media must be heavier/larger than the feed material to achieve breakage, but using

Correspondence concerning this article should be addressed to B. J. Glasser at bglasser@rutgers.edu.

Table 1. Ball Mill Characteristics and Operational Parameters

Mill	Inner diameter (D) (mm)	198
	Length (mm)	162
	Volume (L)	5
	Critical speed (N_c) (rpm)	102
	Operational rotation rate (rpm)	4.3, 17.2, 27.8, 45.2, 56.4
	Operational rotation rate (ϕ_c)	0.04, 0.17, 0.27, 0.44, 0.55
Media	Material	Chrome steel
	Diameter (d_m) (mm)	25.4
	Number	1, 5, 14, 37
	J	0.3, 1.5, 4, 37
	Specific gravity	7.82
Material	Silica sand	
	Specific gravity	2.6
	Material weight (g)	300

excessively heavy/large media results in significant overgrinding, as the increased impact energy from the media weight is much more than is necessary for breakage.[12] Therefore, it is desired to choose the size that will just break the largest particle in the feed.[13] A range of formulas exists relating the size of grinding media (d_m in mm) to the size of the feed material (x_m in mm). Erdem and Ergun[14] cite the classic equation $x_m = Kd_m^2$, where K is an empirically determined constant usually between 10^{-2} and 10^{-3}.[2] Austin et al.[12] enhance the equation by varying the exponent and the empirical constant to fit a variety of grinding experiments, finding that the general theory of the form $x_m = Kd_m^{\alpha}$, holds reasonably well for α between 0.5 and 1. Alternatives to the above equation, that is, $d_m = 28x_m^{1/3}$,[7] $d_m = 6\log(x_p\sqrt{x_m})$,[7] where x_p is the average product particle size in mm and $x_m = 0.2971e^{0.0346d_m}$,[14] also give good agreement with select sets of experimental data. However, it is known that the feed size distribution, feed hardness, mill diameter, specific gravity of the media and the mill rotation rate all affect the ball size selection, and none of the above equations include any parameter except the average feed and product particle size. Bond[13] presents a more comprehensive equation as shown below

$$d_m = \left(\frac{x_m}{K}\right)^{1/2}\left(\frac{SgWi}{100Cs\sqrt{D_m}}\right)^{1/3} \quad (1)$$

where S_g is the specific gravity of the media, Wi is the bond work index of the material to be ground, Cs is the rotation rate of the mill and D_m is the diameter of the mill. Yet, there is still no consensus as to which equation is most reliable. The above equations suggest an optimal media size for a particular application ranging from 5 mm to 100 mm. It is apparent that these equations were empirically developed for specific processes and the range of media sizes suggested is too disparate for legitimate utility. Before a general equation can be developed, it is necessary to understand how breakage mechanisms vary as a function of operating conditions and media size, and ensure that all appropriate variables are included in the analysis.

In this article, we will use a technique called the attainable region (AR) analysis to optimize the production of an intermediate sized product in a batch ball mill. An intermediate sized product is desired because in many industries that handle granular materials, for example, the minerals processing or chemical industry, the existence of very small particles or fines, presents many problems, including possible dust explosions,[15] personnel exposure risks[16] and processing problems.[17,18] Also, the presence of fines in a milling operation leads to a phenomenon known as the cushioning effect.[19–21] Here, the smaller particles fill the voids between the larger particles, and when the larger particle experiences a large enough force, this force is transmitted to the smaller particles resulting in less damage to the larger particle than if it were the only particle in the mill. Also, overgrinding is a significant concern when milling shear and heat-sensitive materials, such as biomaterials, food and pharmaceuticals.[19] As a result, rarely is it the goal to reduce the particle to the smallest size possible. Rather, the desired product is of an intermediate size. Hence, milling operations are a balance between reducing the size of a particle and minimizing overgrinding to maximize efficiency. In addition, in the energy and mineral extraction industries, energy usage is the dominant production cost, as the material is inexpensive and throughput is on the order of tons. In addition, grinding media size has been shown to be one of many parameters controlling the degree of refinement initiating the self-sustaining reaction driving the mechanical alloying and reactive milling process.[22–24] Therefore, the optimization problem is multidimensional, and changes depending on the particular needs of the industry and product. AR analysis is an optimization approach that is flexible enough to handle the various requirements of multiple industries, but robust enough to effectively determine optimal operating parameters from bench scale to production scale.

The AR analysis has been used to optimize comminution operations from a numerical and experimental perspective.[25–28] Khumalo et al.[25,27] theoretically demonstrated and later verified experimentally that the same net energy input did not produce the same product particle size distribution and the AR could be utilized to perform simultaneous process synthesis and optimization. In addition, they extended their work from systems with only milling to those including classification and recycle.[28] Metzger et al.[26] extended the idea and found that the highest yield of a product of intermediate size was achieved when operating at a low rotation rate and a low grinding media fill level and rotation rate could be used as an optimization parameter. They demonstrated the ability of the AR analysis to reduce milling time by up to 50% in addition to suggesting reintroduction of feed material as a means to minimize flow problems when grinding coal to fire power plants. Katubilwa et al.[29] utilized the AR analysis technique in conjunction with a population balance model to track the breakage behavior of coal as a function of grinding media diameter. They found that there was a relatively small variation in breakage for larger grinding media sizes, whereas smaller grinding media sizes increased the yield of fines (<75 μm).

In this article, we will briefly overview the construction of the AR. Next, we will present an investigation of the effect of rotation rate and grinding media fill level with a single size of media and then compare these results with those for a larger size grinding media.

Experimental Approach

The experimental apparatus used in this work is identical to that used by Metzger et al.[26] and is briefly outlined here. Specifics of the apparatus are provided in Table 1, and the apparatus is shown schematically in Figure 1a.

A steel drum of 5 L in volume rotates horizontally on a set of rollers (GlenMills, Clifton, NJ). The specific or

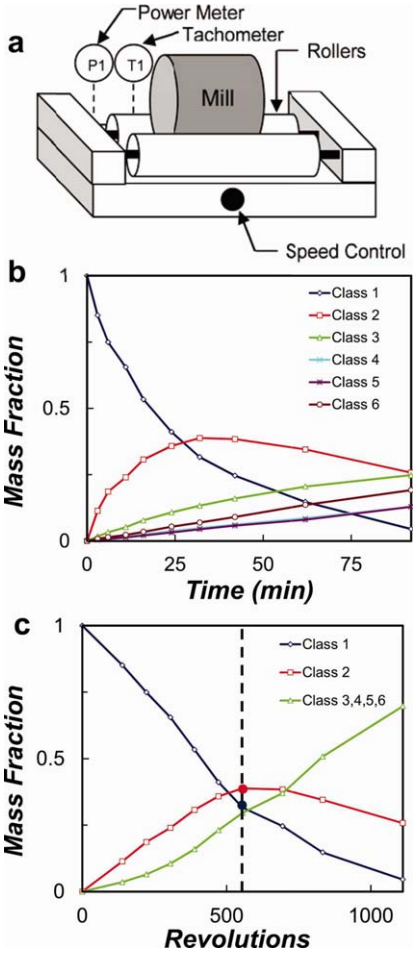

Figure 1. Milling apparatus and data collected.

(a) Schematic of the batch ball mill setup. (b) Mass fraction of each of the six size classes vs. time for $J = 1.5\%$ and $\phi_c = 0.27$. (c) Mass fraction of only the three size classes of interest vs. number of revolutions, showing the number of revolutions selected to produce point X in Figure 2. [Color figure can be viewed in the online issue, which is available at wileyonlinelibrary.com.]

dimensionless rotation rate is represented by $\varphi_c = N/N_c$, which is the rotation rate of the drum, N, relative to the critical rotation rate, N_c, or the point at which the charge begins to centrifuge.[8] This value is calculated empirically using Eq. 2 below

$$N_c = \frac{42.2}{\sqrt{D_m - d_m}} \tag{2}$$

Here D_m is the mill diameter in meters and d_m is the diameter of the grinding media in meters. In our system, N_c is 102 rpm, meaning the minimum and maximum achievable rotation rates are $\varphi_{c,min} = 0.04$ to $\varphi_{c,max} = 0.77$, respectively. Silica sand (FilPro 1/4 × 1/8 in, Superior Pools, Piscataway, NJ) prescreened between 4 and 5.6 mm (sieve size no. 5 and 3 1/2, respectively) is used as the test material in this study. The fractional filling of the drum by grinding media, J, is given by

$$J = \frac{\text{mass of media}/\text{media density}}{\text{mill volume}} \times \frac{1.0}{0.6} \tag{3}$$

Such an empirical equation is used because on the industrial scale, it is easier to estimate the fill height including voids and back that calculate the grinding media weight. The span of particle sizes below 5.6 mm is divided into six distinct size classes as shown in Table 2. The mill loaded with test material and the appropriate level of grinding media is operated for a specified interval and stopped, all material is sieved into and then weighed in the size classes defined in Table 2. Finally, all material is returned to the mill and the process is repeated until adequate grinding is accomplished.

This investigation focuses on the effect of rotation rate (φ_c), grinding media fill level (J), grinding media diameter (d_m) and grinding time (t) on the breakage of particles in a batch ball mill. Specific levels of rotation rate and grinding media fill level used are listed in Table 1. The results presented here are strongly affected by the material being milled, and the main utility of this work lies in the methodology and implementation of that methodology rather than the specific results.

Results and Discussion

We start by presenting results for 25.4 mm grinding media. Figure 1b shows the typical type of data collected from a mill run specifically at $J = 1.5\%$ and $\phi_c = 0.27$. The system begins with 100% of the feed material, or a mass fraction of 1, at time 0. Once the mill begins to rotate, breakage occurs, reducing the material in the feed size class to a smaller size or larger size class number. Eventually, the smaller size classes reach their maximum and then decrease as breakage preferentially selects those larger particles and breaks them into smaller daughter particles. This pattern holds for all size classes until all the material in the mill resides below the upper threshold of size class six.

For our purposes, it is convenient to represent the time element with number of revolutions instead of overall time. In addition, as we are mostly concerned with the optimization of the larger intermediate size class (size class two), we group the undesired smaller size classes together (size class three, four, five and six) to form a single undesired size class. This is shown in Figure 1c. In addition, we use Figure 1c to demonstrate how one constructs the AR from grinding profiles. Simply select a number of revolutions on Figure 1c (the vertical dashed line) and take the intersection with the two size classes of interest (one and two). Then plot these in M_1 vs. M_2 space as shown by point X in Figure 2a. Continue this procedure for each of the number of revolutions to build a curve that begins at the bottom right for 0 revolutions (point F in Figure 2a) and moves in the upper left direction signifying the destruction of size class one (left) and creation of size class two (up). The region under this curve is called the AR. More detail on the construction of the AR can be found in a previous investigation by our group.[26]

One of the powers of the AR is the ability to quickly and effortlessly compare two runs of differing parameters to determine which provides the optimal production of the desired product. An example of this is shown in Figure 2 for

Table 2. Size Classes

Size Class	Size Range (μm)
One	5600–4000
Two	4000–2000
Three	2000–1000
Four	1000–600
Five	600–300
Six	<300

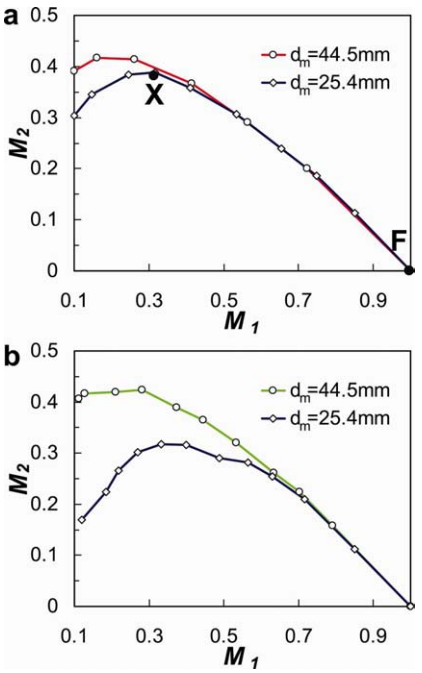

Figure 2. Comparison between larger and smaller media at otherwise identical operating parameters.

(a) $J = 1.5\%$ and $\phi_c \sim 0.25$ (b) $J = 10.7\%$ and $\phi_c \sim 0.25$. [Color figure can be viewed in the online issue, which is available at wileyonlinelibrary.com.]

two runs at almost identical conditions, only differing in the size of grinding media used and the grinding media fill level. The results for the 44.5 mm grinding media are taken from previous work.[26] The higher the plot reaches on the vertical axis, the more optimal the run. Therefore, for each of the operating conditions presented in Figure 2, the larger media ($d_m = 44.5$ mm) produce more of the desired product. Starting at point F and advancing towards point X, each of the plots follow the same trajectory initially. However, as the curves approach their maxima they deviate. Interestingly, the situation in Figure 2b shows a large discrepancy between the amounts of the desired product produced using the two sizes of grinding media, whereas the conditions in Figure 2a have little difference between the two cases. One can also utilize the AR presentation to identify selectivity, that is, how much of the desired product is produced from the starting material. In Figure 2, the selectivity to size class two from size class one is always greater for the larger grinding media. Figure 2 shows that the grinding media size do affect the distribution of sizes produced by breakage, and therefore, the assumption that grinding media size does not need to be included in design and scale-up equations needs to be reconsidered. In Figures 2a, b the dimensionless rotation rate, ϕ_c, is constant for the large and small grinding media, but it should be noted that the actual dimensional rotation rates, N, for each case are slightly different as the size of the smaller media slightly alters the critical rotation rate (N_c: rotation rate at which the media begin to centrifuge). However, the difference is only 6%.

Investigations were performed at multiple combinations of rotation rate and grinding media fill level to quantify breakage as a function of operating conditions. The goal was to span the entire M_2 vs. M_1 mass fraction phase space to determine which runs produced the most amount of the desired product: size class two. First, an investigation was performed at a constant grinding media fill level and variable rotation rate. Figure 3 presents a typical result (constant $J = 1.5\%$) demonstrating a monotonic trend of increased production of the desired product as you decrease the rotation rate at a constant grinding media fill level. This trend was also observed for $J = 4.0\%$ and is similar to what was observed by Metzger et al.[26] At these grinding media fill levels, decreasing the rotation rate reduces the total energy delivered to the particle bed, minimizing overgrinding, more efficiently producing material of the desired size. We note that our current experimental setup does not allow us to operate at a rotation rate lower than $\phi_c = 0.04$. However, one would expect no breakage at $\phi_c = 0$. There is therefore an optimal rotation rate (somewhere between $\phi_c = 0.04$ and $\phi_c = 0$) that would maximize production of size class two.[26] For higher rotation rates, $\phi_c > 0.27$, the AR profiles differ only slightly, suggesting that below a certain drum rotation rate there is a transition in the internal flow dynamics. Also, all profiles are essentially indistinguishable for $M_1 > 0.7$, agreeing with results previously obtained for the larger media.[26]

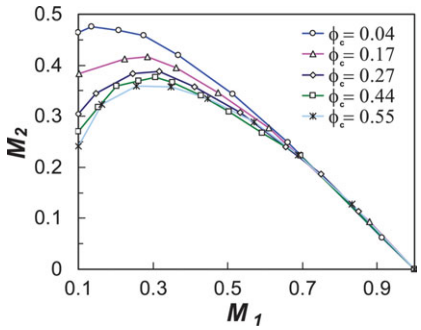

Figure 3. Mass fraction of size class two vs. mass fraction of size class one for various rotation rates at a grinding media fill level of $J = 1.5\%$.

[Color figure can be viewed in the online issue, which is available at wileyonlinelibrary.com.]

Figure 4 presents the same data in a commonly encountered representation for experimental results in the size reduction field,[2,8] that is, the data are presented in cumulative percent passing format and each curve represents a single point on the AR, specifically the distributions at the

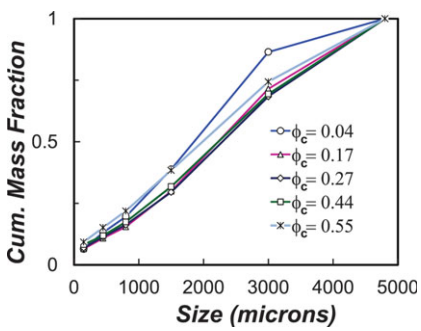

Figure 4. An alternative representation of the data in Figure 3, at $J = 1.5\%$.

Cumulative percent passing plots at the maximum production of M_2 for each case in Figure 3. [Color figure can be viewed in the online issue, which is available at wileyonlinelibrary.com.]

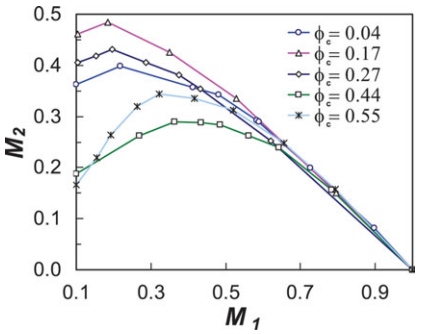

Figure 5. Mass fraction of size class two vs. mass fraction of size class one for various rotation rates at a grinding media fill level of $J = 0.3\%$.

[Color figure can be viewed in the online issue, which is available at wileyonlinelibrary.com.]

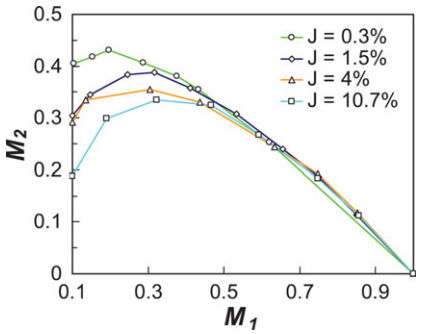

Figure 6. Mass fraction of size class two vs. mass fraction of size class one for various levels of 25.4 mm grinding media at a single speed ($\phi_c = 0.17$). $J = 0.3\%$ represents one grinding media, $J = 1.5\%$ represents five grinding media, $J = 4\%$ represents 14 grinding media, and $J = 10.7\%$ represents 37 grinding media.

[Color figure can be viewed in the online issue, which is available at wileyonlinelibrary.com.]

optimum M_2 points in Figure 3. This presentation with more than one run at multiple time points is an extremely busy plot, making comparisons difficult. With this presentation, it is possible to visualize the overall particle size distribution, but determining the conditions that produce the maximum amount of size class two can be misleading, as the points at the larger particle sizes are dependent on the amount of particles in the lower size classes due to the cumulative nature of the plot. In Figure 4, this can be seen by tracking the amount of material at or below 3000 μm (the average particle size of size class two) for the different rotation rates. One observes that for material at or below 3000 μm the curves are ordered from highest to lowest as follows: ϕ_c = 0.04, 0.55, 0.17, 0.44, 0.27. However, from Figure 3 (where size classes are plotted), the rotation rate that optimizes size class two does not follow this ranking and instead is ordered as follows (from best to worst): ϕ_c = 0.04, 0.17, 0.27, 0.44, 0.55.

The idea of using size classes to represent the data is not exclusive to the AR analysis and researchers carrying out population balances[30] divide the continuous size distribution into discrete size classes and track them as a function of mill operation. Researchers then model the birth and death of particles into and out of each size class, but then attempt to reproduce the experimental continuous particle-size distributions as their final results.[31] In our view, utilizing size classes to examine experimental results enables simple determination of optimal milling conditions independent of the population balance model framework and the AR naturally follows as an easy and understandable presentation of the most pertinent information to determine optimal operating conditions.

Figure 5 presents data for $J = 0.3\%$ that does not follow the trend shown in Figure 3 and demonstrates nonmonotonic behavior when decreasing the grinding media fill level. An intermediate grinding media fill level, $\phi_c = 0.17$ in this case, achieves the largest maximum of M_2, whereas operation at lower and higher rotation rates yields less of the desired product. For the first time using our experimental equipment, the parameter combination that yields the most of the desired product does not reside at the limits of our experimental equipment. In addition, when operating at the highest rotation rate, there is a slight increase in the amount of desired product produced, compared to the next highest rotation rate investigated. This situation may produce more of the desired product, but is undesirable from an energy perspective, requiring 46% more energy than the $\phi_c = 0.27$ case, which also yields 25% more of the desired product. Therefore, we have identified a situation where the macroscopic operational parameters affect the resultant breakage, presumably through changes to the microscopic flow and breakage behavior inside the mill.

Alternative investigations were performed holding the rotation rate constant and varying the grinding media fill level. Similar results were seen. In some cases, the standard, monotonic trends of the amount of desired product increasing with decreasing grinding media fill level were seen, as shown in Figure 6 for $\phi_c = 0.17$. Once again, the limits of our experimental equipment have been reached as there will inevitably be a fill level between 0 and $J = 0.3\%$ that produces optimal breakage. A rotation rate of $\phi_c = 0.27$ also demonstrates the same monotonic trend.

The remaining rotation rates demonstrate new, nonmonotonic trends as shown in Figure 7 for $\phi_c = 0.44$. Now an intermediate grinding media fill level yields the highest amount of size class two at this rotation rate, $\phi_c = 0.44$ and $J = 4.0\%$. Therefore, as seen with the drum rotation rate, the limit of the previous suggestion to decrease the amount

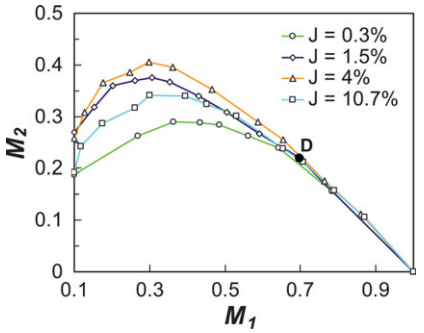

Figure 7. Mass fraction of size class two vs. mass fraction of size class one for various levels of 25.4 mm grinding media at a single speed ($\phi_c = 0.44$).

***D* represents the point of deviation of the curves.**

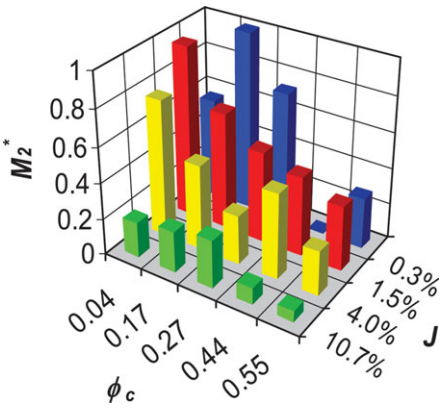

Figure 8. Optimal production of M_2 for each combination of J and ϕ_c.

Here, M_2 is scaled to span the range from 0 to 1.[Color figure can be viewed in the online issue, which is available at wileyonlinelibrary.com.]

of grinding media to achieve the most of size class two has also been reached. This behavior is also encountered for $\phi_c = 0.55$ and 0.04, though the optimal amount of grinding media varies for each case.

Optimal production of M_2 from all combinations of rotation rate (ϕ_c) and grinding media fill level (J) is shown in Figure 8 for the 25.4 mm media. These values are determined by selecting the maximum mass fraction of M_2 attained by each combination of J and ϕ_c in Figures 3 and 5–7 and the remainder of the J and ϕ_c combinations we have examined (not shown). In addition, M_2 is scaled (M_2^*) by its highest and lowest value achieved to span the range from 0 to 1. A value of unity corresponds to the overall maximum mass fraction of M_2 achieved of 0.48 for $J = 0.3\%$ and $\phi_c = 0.17$, and a value of zero corresponds to the lowest optimal mass fraction of M_2 achieved of 0.29 for $J = 0.3\%$ and $\phi_c = 0.44$. For example, the data presented in Figure 4 is represented by the $J = 0.3\%$ row of columns in blue at the back of Figure 8. Generally, the largest mass fraction of size class two is obtained for lower combinations of J and ϕ_c, though the lowest combination ($\phi_c = 0.04$ and $J = 0.3\%$), does not follow this trend and yields an optimal mass fraction of M_2 10–20% lower than its immediate neighbors.

When looking at the optimal J level for a given rotation rate (rows of columns going into the page in Figure 8), we see a complex relationship. Starting at the lowest rotation rate ($\phi_c = 0.04$), an intermediate grinding media fill level ($J = 1.5\%$) produces most of the desired size class. An increase in the rotation rate to $\phi_c = 0.17$ and $\phi_c = 0.27$ exhibits a maximum at the lowest value of $J = 0.3\%$. A further increase in the rotation rate shifts the optimum to $J = 4.0\%$ and $J = 1.5\%$ for $\phi_c = 0.44$ and $\phi_c = 0.55$, respectively. Overall, the maxima presented by the higher rotation rates are well below those achieved with the lower rotation rates.

In terms of choosing the optimal rotation rate at a given grinding media fill level (columns moving left to right in Figure 8), the situation is similar. For the lowest level of grinding media investigated ($J = 0.3\%$), the maximum amount of M_2 produced occurs at an intermediate rotation rate of $\phi_c = 0.17$, and is the global maximum for this size grinding media. For grinding media fill levels of $J = 1.5\%$ and $J = 4\%$, the optimal production of size class two occurs at the lowest rotation of $\phi_c = 0.04$. Further increasing the amount of grinding media in the mill to $J = 10.7\%$ shifts the optimal production of size class two to an intermediate rotation rate of $\phi_c = 0.27$, yet this maximum is much less than those obtained for the other J levels. For reference, a similar plot for the larger 44.5 mm media would have the highest point at the lowest parameter combination of $J = 1.5\%$ and $\phi_c = 0.03$ and descend to lower values of M_2 max at all other J and ϕ_c.

Presumably, a shift in flow and breakage behavior is occurring as the rotation rate and grinding media fill level varies. Operation at the lowest rotation rate and grinding media fill level ($J = 0.3\%$ and $\phi_c = 0.04$) contributes the least amount of energy to the milling process, whereas the largest amount of energy is contributed at $J = 10.7\%$ and $\phi_c = 0.55$. Obviously, the trends in Figure 8 demonstrate that there is a nonlinear relationship between the production of size class two and energy input. Ideally, production of size class two would proceed following a cleavage-type breakage mechanism, where the initial feed particles split into multiple particles falling in size class two, without producing fines. Such a scenario is not observed here and is generally difficult to achieve, as many factors affect how rotational energy is converted into breakage. First, not every contact produces breakage, as some collisions do not exceed the inherent strength of a particle, and simply result in elastic deformation and translational motion without breakage.[32] For the lowest parameter combination of $J = 0.3\%$ and $\phi_c = 0.04$, the contacts between the grinding media and material may not be energetic enough to produce sufficient breakage, possibly leading to the reduction in the amount of desired product produced. Second, even if the average collision is energetic enough to cause breakage, contacts between grinding media and between grinding media and the mill shell do not contribute to the production of desired product, but squander usable energy to contacts that only produce excess noise, heat and wear of mill parts and no breakage. Both of these types of collisions are inefficient as energy delivered to the mill is used, but does not produce breakage. Similar arguments hold for operation at the higher grinding media fill levels due to the increased chance of grinding media—grinding media contacts and contacts between the grinding media and the mill shell. Such an occurrence may explain the lower maxima obtained at higher rotation rates of $\phi_c = 0.44$ and $\phi_c = 0.55$. Finally, perfect breakage following the cleavage mechanism is a rarity, with fines almost always produced through abrasion or massive fracture. The wide distribution of contact energies present in a mill essentially ensures the occurrence of overgrinding, diminishing expectations for the overall maximum amount of M_2. However, it may be possible to tune the operational parameters to promote more efficient breakage, which may occur for the parameter combinations at lower values of J and ϕ_c. For example, at the lowest grinding media fill level, an increase in the rotation rate from $\phi_c = 0.04$ to $\phi_c = 0.17$ increases the production of M_2. This increase contributes additional energy to the media, which may help the contacts eclipse the energy needed to more consistently fracture the feed particles. Further increasing the rotation rate results in a decrease in the production of M_2, possibly a result of an increase in the amount of inefficient contacts between the grinding media and the wall, decreasing the energy with which the grinding media contact the particles. Corresponding arguments can be drawn along additional "slices" through Figure 8 to present

arguments as to how energy, contact type and breakage type contribute to the production of the desired product.

A broad range of conditions was explored in this academic investigation to fully characterize the breakage behavior, but the level of detail that should be carried out in practice will depend on the value to the company or application. We have used the AR to determine when a maximum of M_2 is achieved, examining a large range of parameters. However, the AR approach can be used to quickly collect information about a system without running all parameter combinations. This procedure to reduce experimentation will work as long as milling trajectories on the AR plot do not cross. In the cases we have examined, milling trajectories (within experimental error) do not cross. To illustrate this procedure to reduce experimentation, we start with the information presented in Figure 7, where 471 min or almost 8 h of mill operation was required to collect all of the data. However, we could have determined the conditions to maximize the production of size class two in much less time using the AR analysis. In particular, the two runs at the largest grinding media fill level ($J = 10.7\%$ and 4.0%) require the least amount of run time, and therefore the investigation should begin by running these to completion ($M_1 \sim 0.1$) as shown in Figure 7, requiring 23 min of mill operation. As shown by Metzger et al.[26] there is little difference between the particle size distributions when the AR plots overlap, even if they are obtained by operating at different conditions. In our work, we have seen that the initial trajectories often overlap as size class one is broken into size class two. We can see this in Figure 7 where starting from the feed point ($M_1 = 1.0$, $M_2 = 0.0$) all curves overlap up until point D (the point of divergence).

As the goal is to determine the conditions that yield the most of the desired intermediate product, we can continue the remaining runs ($J = 1.5\%$ and 0.3%) for a limited number of time points beyond point D. We can then compare their trajectories to the run that yields the most of the desired product ($J = 4.0\%$), the current champion. If a run extends the AR, that is, has a slope greater than that of the current champion, then it should be continued to completion to determine the maximum amount of M_2 achievable. If the slope falls below that of the current champion, then the run can be abandoned, as it will not eclipse the maximum of the current champion. For the case of the data presented in Figure 7, neither of the two lower grinding media fill levels ($J = 1.5$ and 0.3%) have slopes at point D larger than that of the $J = 4.0\%$ case, so they could have been abandoned slightly beyond point D. As a result, the time required to complete these runs is not necessary (347 min), and thus the total time savings is 347 min or 74% of the original run time. We term this procedure smart experimentation and it can be utilized in most situations where a single variable is varied while holding all others constant to reduce the time required to explore the parameter space. The procedure increases the practical utility of the AR approach when a specific objective function is known.

Returning to one of the original goals of the investigation, the overall optimal profiles producing the largest amount of size class two for each of the two grinding media sizes is shown in Figure 9. All other parameter combinations not shown do not produce as much M_2 with the entire AR falling within those shown in Figure 9a, and are therefore not considered in this analysis. Grinding with the larger media at

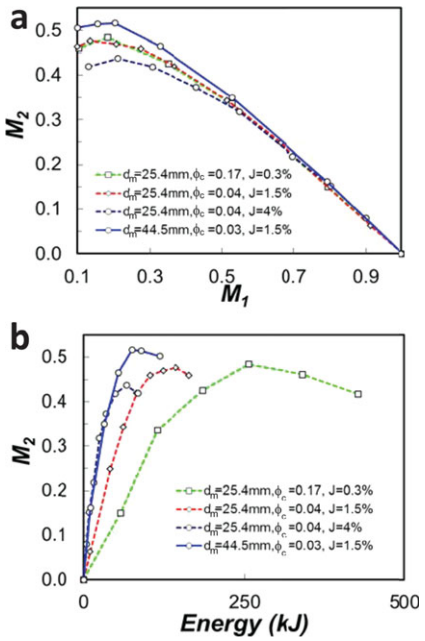

Figure 9. Overall optimal production of M_2 from both media sizes, (a) vs. M_1 and (b) vs. energy.

[Color figure can be viewed in the online issue, which is available at wileyonlinelibrary.com.]

the lowest fill level and the lowest amount of the grinding media yields the most amount of desired product ($d_m = 44.5$ mm, $\phi_c = 0.03$ and $J = 1.5\%$). This is in agreement with findings in classical milling texts, such as Austin et al.[8] and recent experimental results,[9] where large media are used to produce more of a coarser product. This policy should be used if production of an intermediate sized product is the primary process goal. As mentioned previously, there must be a point at which this trend no longer continues as a rotation rate of zero would not produce breakage. Nonetheless, we have shown that there is a complex interplay between grinding media size, rotation rate, and amount of grinding media to produce the most of a desired intermediate product.

Looking at Figure 9a, the next closest runs utilize the smaller media at various settings of rotation rate and grinding media fill level and seem to be acceptable alternatives from a desired product perspective. However, if the AR is reconstructed using the energy consumption of each process as a second constraint to the process (Figure 9b), these runs seem less attractive. As shown in Figure 9b, the most optimal run with the smaller media requires more energy (over three times more) than the overall optimal run, while producing slightly less product (~7% less). Therefore, for industries where energy costs are significant contributors to overall operating costs, it makes even more sense to operate with the larger media at the optimal conditions. All other runs with the larger amounts of grinding media ($J > 4\%$) use much less energy than the runs with the smaller amounts of grinding media, but do not achieve as much of the desired product as the run with the larger grinding media at the slowest rotation rate and the lowest level of grinding media (not shown). In addition, operation at the largest input energy level investigated with the small media achieves a maximum well below the other cases.

Until now, the objective function has been to optimize the production of size class two. However, there are many other

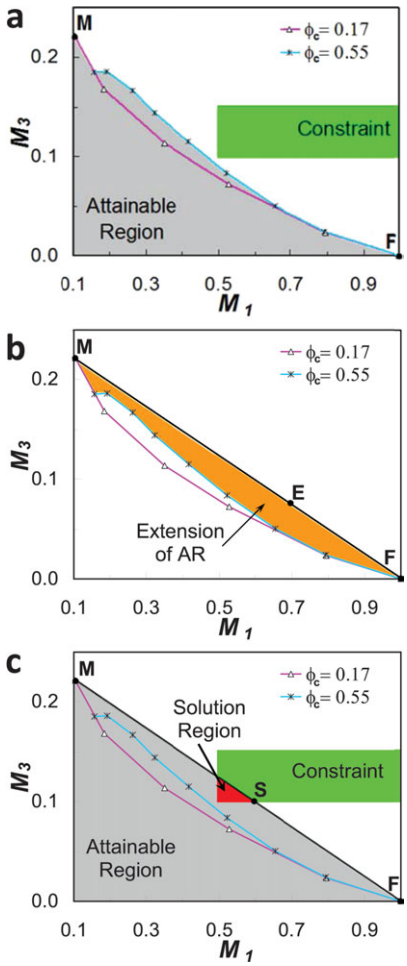

Figure 10. Optimization of a particle size distribution.

(a) Preliminary AR for $J = 0.3\%$ and the region satisfying the constraint (b) extended AR achieved through mixing (c) solution satisfying the presented constraints. [Color figure can be viewed in the online issue, which is available at wileyonlinelibrary.com.]

scenarios encountered across the comminution industry that the AR analysis is capable of optimizing. Consider the scenario where the desired product is of a smaller size but due to the many difficulties associated with smaller particles, you also require an amount of larger particles to limit the influence of the fines on the flow and characteristics of the product. An example of such a scenario is encountered when preparing coal feed stocks to fire power plants, where you desire a small particle size for a consistent burn, but also need larger particles to prevent flow stoppages due to cohesion of the small particles. In this scenario, the fines are material collected in size class three and the coarse material is that in size class one. To be more specific, it is desired to have a mass fraction of size class three between 0.1 and 0.15 and a mass fraction of size class one no less than 0.5 in the final product. This example will be used to demonstrate the power of the AR analysis to recommend optimal operating conditions for problems where the solution is not readily apparent.

Shown in Figure 10 is the AR for the situation outlined above. The data used to construct this AR is identical to that used previously, the only difference being M_3 is plotted vs. M_1 instead of M_2, because we now wish to optimize the amount of M_3 in the product. Two representative grinding profiles are shown in Figure 10a. The grinding profiles start at a mass fraction of $M_1 = 1$, represented by point F. As grinding begins, material in M_1 is broken mostly into M_2, with a small amount of material collected in M_3, resulting in a very modest increase in the amount of M_3 collected. Then, further grinding breaks the remaining M_1 and more plentiful M_2 into M_3 at an accelerated rate, resulting in a concavity in the boundary of the AR as it approaches its maximum at point M in Figure 10a. Only two curves are shown for simplicity. All other curves have slightly different shapes and maxima, but generally the same behavior, falling underneath or on top of the curves presented here.

If we were to apply the constraints of the new process, specifically $0.1 < M_3 < 0.15$ and $M_1 > 0.5$, we see that the AR, as presented, cannot achieve such a particle size distribution, as demonstrated by the lack of an intersection between the region satisfying the constraint and the AR in Figure 10a. However, the concavity in the boundary of the AR presents an opportunity for a possible solution to this problem. A characteristic of the AR, as demonstrated previously,[26,33] is that two points in phase space can be linearly connected and such an operation represents the mixing of the two products at both ends of the line. For example, a mixing line is drawn in Figure 10b connecting the feed point F with the maximum amount of M_3 produced, point M. All points along the line represent various particle size distributions that can be achieved by mixing product from the two terminus points in some proportion. This proportion is determined using the Lever arm rule.[34] If the goal is to achieve a particle size distribution at point E in Figure 10b, the line $\overline{FM}$ would be split into two sections $\overline{FE}$ and $\overline{EM}$. The length of $\overline{EM}$ relative to the total length of $\overline{FM}$ corresponds to the amount of fresh feed that must be mixed with the product at point M. In this case, $\overline{EM}$ is 66% of the total length, so point E is obtained by creating a mixture containing 33% material collected out of a mill operating to point M and 66% of fresh feed material from point F. Important to note and not altogether obvious is that this point is achieved by mixing additional feed material with product to achieve the desired particle size distribution. In chemical reaction engineering terminology, this is referred to as feed bypass. Also essential is that now the AR is extended to include the shaded region above the grinding profiles and below the mixing line. The process can be repeated to achieve any point within the shaded region in Figure 10b, referred to as the extended AR.

Returning to the new constraints, we can follow the same procedure and determine if feed bypass is capable of satisfying the presented design problem. Figure 10c shows the new AR including the extended region, as well as the region satisfying the constraints of the design problem. One can now see that there is a region of overlap between the constraints and the AR, and thus the process is capable of achieving the desired particle size distribution. To achieve point S shown in Figure 10c, one would operate the mill to point M, and then prepare a mixture of 45% product from point M and 55% of fresh feed to yield a product meeting the prescribed requirements. The above example details an analysis that quantitatively yields a solution to a range of design problems without requiring any additional experimentation. Such an analysis demonstrates the flexibility and power of the AR analysis to optimize a variety of comminution design objectives.

Conclusion

Using the AR approach as an easy and understandable way to present milling results, we have shown that though not often cited in many design and scale-up equations, the size of grinding media is an important parameter in optimal operation of batch ball mills. Large or relatively minor discrepancies in optimal production of a product of intermediate size may occur, and the situation varies with both the drum rotation rate and the grinding media fill level. Contrary to results obtained in previous investigations with larger media, certain combinations of rotation rate and grinding media fill level produce nonmonotonic behavior as one parameter is held constant and the other varied. Also presented was a procedure to reduce the time required to explore the parameter space and identify optimal conditions that satisfy an objective function. Therefore, close control of all parameters is necessary when attempting to improve the efficiency of grinding processes. We have carried out a limited set of experiments for one material, and therefore further work is required to expand the operating conditions, explore the effect of additional media sizes and to investigate if similar trends are observed with other materials. Finally, investigations are in progress from a numerical approach to classify the type of breakage occurring in the mill and connect the microscopic breakage mechanism to the macroscopic operating conditions.

Acknowledgments

The authors thank J. Selvaggio, S. Larisegger and H. Pücher for their assistance. This work was partly funded by the National Science Foundation.

Literature Cited

1. Morrison RD, Cleary PW. *The road towards a virtual comminution machine*. In: *4th International Conference on DEM*, Brisbane, Australia, 2007:1–12.
2. Lowrison GC. *Crushing and Grinding: The Size Reduction of Solid Materials*. Cleveland, Ohio: CRC Press, 1974.
3. Fuerstenau DW, Abouzeid AZM. The energy efficiency of ball milling in comminution. *Int J Miner Process*. 2002;67:161–185.
4. Varinot C, Hiltgun S, Pons M-N, Dodds J. Identification of the fragmentation mechanisms in wet-phase fine grinding in a stirred bead mill. *Chem Eng Sci*. 1997;52:3605–3612.
5. Lynch AJ. *Mineral Crushing and Grinding Circuits*. New York: Elsevier, 1977.
6. Mishra BK. A review of computer simulation of tumbling mills by the discrete element method: part II—practical applications. *Int J Miner Process*. 2003;71:95–112.
7. Bernotat S, Schonert K. *Size Reduction*. Weinheim: VCH Verlagsgesellschaft, 1988.
8. Austin LG, Klimpel RR, Luckie PT. *Process Engineering of Size Reduction: Ball Milling*. New York: American Institute of Mining, Metallurgical, and Petroleum Engineers, 1984.
9. Orumwense AO. Effect of media type on regrinding with stirred mills. *Miner Metall Process*. 2006;23:40–44.
10. Samanli S, Cuhadaroglu D, Hwang JY. An investigation of particle size variation in stirred mills in terms of breakage kinetics. *Energy Sources Part A: Recovery Utilization Environ Eff*. 2011;33:549–561.
11. Prasad DVN, Theuerkauf J. Effect of grinding media size and chamber length on grinding in a spex mixer mill. *Chem Eng Technol*. 2009;32:1102–1106.
12. Austin LG, Shoji K, Luckie PT. The effect of ball size on mill performance. *Powder Technol*. 1976;14:71–79.
13. Bond FC. Crushing and grinding calculations. Part I. *Br Chem Eng*. 1961;6:378–385.
14. Erdem AS, Ergün SL. The effect of ball size on breakage rate parameter in a pilot scale ball mill. *Miner Eng*. 2009;22:660–664.
15. Shelley S. Preventing dust explosions. *Chem Eng Prog*. 2008;104:8–14.
16. Ghadiri M, Zhang Z. Impact attrition of particulate solids. Part 1: a theoretical model of chipping. *Chem Eng Sci*. 2002;57:3659–3669.
17. Roche O, Gilbertson MA, Phillips JC, Sparks RSJ. The influence of particle size on the flow of initially fluidised powders. *Powder Technol*. 2006;166:167–174.
18. Abou-Chakra H, Tüzün U. Microstructural blending of coal to enhance flowability. *Powder Technol*. 2000;111:200–209.
19. Bilgili E, Scarlett B. Population balance modeling of non-linear effects in milling processes. *Powder Technol*. 2005;153:59–71.
20. Bilgili E, Yepes J, Scarlett B. Formulation of a non-linear framework for population balance modeling of batch grinding: beyond first-order kinetics. *Chem Eng Sci*. 2006;61:33–44.
21. Bilgili E. On the consequences of non-first-order breakage kinetics in comminution processes: absence of self-similar size spectra. *Part Part Syst Charact*. 2007;24:12–17.
22. Jiang X, Trunov MA, Schoenitz M, Dave RN, Dreizin EL. Mechanical alloying and reactive milling in a high energy planetary mill. *J Alloy Comp*. 2009;478:246–251.
23. Chen W, Schoenitz M, Ward TS, Dave RN, Dreizin EL. Numerical simulation of mechanical alloying in a shaker mill by discrete element method. *KONA Powder Part*. 2005;23:152–162.
24. Ward TS, Chen W, Schoenitz M, Dave RN, Dreizin EL. A study of mechanical alloying processes using reactive milling and discrete element modeling. *Acta Mater*. 2005;53:2909–2918.
25. Khumalo N, Glasser D, Hildebrandt D, Hausberger B, Kauchali S. The application of the attainable region analysis to comminution. *Chem Eng Sci*. 2006;61:5969–5980.
26. Metzger MJ, Glasser D, Hausberger B, Hildebrandt D, Glasser BJ. Use of the attainable region analysis to optimize particle breakage in a ball mill. *Chem Eng Sci*. 2009;64:3766–3777.
27. Khumalo N, Glasser D, Hildebrandt D, Hausberger B. An experimental validation of a specific energy-based approach for comminution. *Chem Eng Sci*. 2007;62:2765–2776.
28. Khumalo N, Glasser D, Hildebrandt D, Hausberger B. Improving comminution efficiency using classification: an attainable region approach. *Powder Technol*. 2008;187:252–259.
29. Katubilwa FM, Moys MH, Glasser D, Hildebrandt D. An attainable region analysis of the effect of ball size on milling. *Powder Technol*. 2011;210:36–46.
30. Austin LG. Introduction to the mathematical description of grinding as a rate process. *Powder Technol*. 1971;5:1–17.
31. King RP. *Modeling and Simulation of Mineral Processing Systems*. Boston: Butterworth Heinemann, 2001.
32. Cleary PW. Recent advances in DEM modelling of tumbling mills. *Miner Eng*. 2001;14:1295–1319.
33. Metzger MJ, Glasser BJ, Glasser D, Hausberger B, Hildebrandt D. Teaching reaction engineering using the attainable region. *Chem Eng Educ*. 2007;41:258–264.
34. Geankoplis CJ. *Transport Processes and Unit Operations*, 3rd ed. Englewood Cliffs, NJ: Prentice Hall PTR, 1993.

Manuscript received Jan. 17, 2011, and revision received Sept. 22, 2011.